Theoretical analysis of actual surfaces: The effect on the nematic orientation

L. R. Evangelista and G. Barbero*
Departamento de Física, Fundação Universidade Estadual de Maringá, Avenida Colombo, 3690-87020 Maringá, Paraná, Brazil
(Received 30 November 1992)

The effect of noise on the average orientation imposed by the surface treatment on the bulk properties of a nematic liquid crystal is evaluated. The general solution of the elastic problem in terms of propagators is given. The analysis shows that a nonuniform easy axis requires a careful experimental determination of the anchoring energy, detected by means of optical methods. Several particular cases are analyzed in the strong- and weak-anchoring situations.

PACS number(s): 61.30.Gd, 68.10.Cr

I. INTRODUCTION

The physical description of nematic liquid crystals is made by introducing a director field **n**. It coincides with the average molecular orientation of the molecules forming the phase. As it is well known [1], **n** defines the optical axis of the uniaxial nematic material. Because the usual nematic liquid crystals are not ferroelectric **n** and $-\mathbf{n}$ are equivalent. Only the direction of **n** is physically meaningful. It follows that the physical properties of a nematic sample depend on the spatial distribution of **n**. The director can be written in terms of two polar angles [2] ϕ and ψ. In the event in which **n** is everywhere parallel to a plane, it may be written in terms of one angle only. According to the actual situation this angle is called the tilt or twist angle [3].

To evaluate the director field **n** or ϕ and ψ, the basic principle of the continuum theory is used. This principle states that the actual vector field **n** has to be deduced by minimizing the total elastic energy of the nematic sample. The total elastic energy is a functional of **n** and contains two terms. One is due to the elastic properties of the nematic phase and it depends on the spatial derivatives of **n** and eventually on the applied fields, and it is a bulk term [4]. Another one, due partially to the direct interaction between the surface and the nematic phase and to the broken symmetry introduced by the presence of the surface, which is a surface term [5].

In the absence of external fields **n** depends only on the surface treatment. If a nematic slab is considered and the surface treatment ensures uniform tilt or twist angle, in the bulk, the tilt or twist angle is expected to depend only on the distance of the point considered from the two limiting plates. In this situation, by analyzing some physical properties of the sample, as the optical transmittance or the electric capacitance, it is possible to deduce information on the elastic constants, anisotropies, or the surface properties of the nematic phase [6–10]. Of course the above-described situation is ideal in the sense that never the surface treatment may ensure a perfect uniform orientation of the director. Hence, in our opinion, it is important to know the influence of the nonuniformity of the surface treatment on the experimentally detected quantities as, for instance, the optical-path difference. In the following we will show that the presence of inhomogeneity in the surface treatment could induce experimentalist to a wrong estimation of the surface energy.

Our paper is organized as follows. In Sec. II the general equations governing the tilt angle are deduced and a few important cases of surface misalignment discussed. One of these cases is considered, as an example, in Sec. III, in which the presence of a periodic fluctuation on the average orientation is analyzed in details. In Sec. IV the solution for the tilt angle is given in a general form in terms of propagators. Other typical cases of surface misalignment relevant to periodic fluctuation of surface tilt angle around a mean value are considered in Sec. V, where the strong and weak situations are analyzed. In Sec. VI, the case in which the surface fluctuation around the average tilt angle is a stochastic function is studied, and the physical consequences are evaluated. The main conclusions of our paper are reported in Sec. VII.

II. GENERAL EQUATIONS

Let us consider a nematic slab of thickness d. The Cartesian reference frame is chosen with the z axis normal to the bounding plates, located at $z=\pm d/2$. The x axis is parallel to the direction along which the surface tilt angle is expected to change. In the following, we suppose that the tilt angle ϕ, made by the nematic director with the z axis, is y independent (Fig. 1). In the one constant approximation $K_1=K_3$, the bulk energy density due to the elastic distortion is [2] $f_b=\frac{1}{2}K(\nabla\phi)^2$, where $\nabla\phi=\mathbf{i}(\partial\phi/\partial x)+\mathbf{k}(\partial\phi/\partial z)$. **i** and **k** are the unit vectors parallel to the x and z axes, respectively. We consider, in our paper, the effect of the surface on the orientation of the nematic liquid crystal. The surface energy will be assumed to be of the kind proposed by Rapini and Papoular [11], i.e., $f_s=(W/2)(\phi-\Phi)^2$. In the previous formula, W is the anchoring strength and Φ the easy direction imposed by the surface [11]. The strong-anchoring case corresponds to $W\to\infty$. In this frame, the total energy of the nematic sample, per unit length along the y axis, is given by the functional

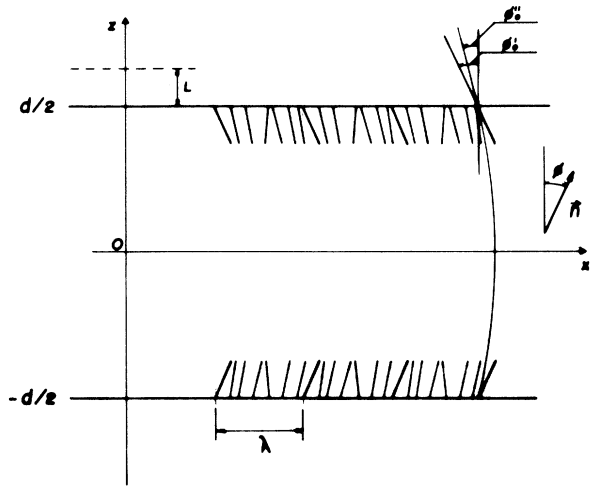

FIG. 1. A nematic-liquid-crystal sample in an antisymmetric arrangement. The actual easy direction, characterized by strong anchoring, is assumed to be a periodic function of x of wavelength λ and amplitude ϕ_0. The x dependence of the tilt angle ϕ disappears for $|z-d/2|$ of the order of a few λ. ϕ_0' is the experimentally detected easy axis, whereas ϕ_0'' is the actual macroscopic tilt angle. L is the measured effective extrapolation length. In this case the local extrapolation length is zero (due to the strong-anchoring hypothesis).

$$F[\phi(x,z)] = \int_{-\infty}^{+\infty} dx \int_{-d/2}^{+d/2} dz \tfrac{1}{2} K(\nabla\phi)^2 + \int_{-\infty}^{+\infty} \tfrac{1}{2}\{W_-[\phi_-(x)-\Phi_-(x)]^2 + W_+[\phi_+(x)-\Phi_+(x)]^2\} dx \ . \quad (1)$$

In (1) the first term represents the bulk contribution, whereas the second one the surface contribution. In (1) $\phi\pm(x)=\phi(x,\pm d/2)$, i.e., $\phi\pm(x)$ are the actual values of the tilt angle at the boundaries $z=\pm d/2$. Furthermore, $\Phi_\pm(x)$ are the easy tilt angles characterizing the lower $(-)$ and upper $(+)$ surface. The director profile, or the function $\phi(x,z)$, is deduced by imposing that the actual deformation minimizes the total elastic energy given by (1). By minimizing (1), standard calculations [12] give

$$\frac{\partial^2\phi}{\partial x^2}+\frac{\partial^2\phi}{\partial z^2}=0, \quad -\infty<x<\infty, \quad -\frac{d}{2}\le z\le\frac{d}{2} \quad (2)$$

for the bulk equation and

$$\pm L\left[\frac{\partial\phi}{\partial z}\right]_{z=\pm d/2}+\phi_\pm(x)-\Phi_\pm(x)=0 \quad (3)$$

for the boundary conditions. In (3) $L=K/W$ is the so-called extrapolation length [13]. In the case of strong anchoring $L=0$, the boundary conditions (3) reduce to

$$\phi_\pm(x)=\Phi_\pm(x) \ , \quad (4)$$

as expected. The nematic orientation inside the sample is then the solution of Eq. (2) satisfying boundary conditions (3) or (4). When $\phi(x,z)$ is known, the physical properties of the nematic sample can be deduced. In the case in which a linear polarized beam impinges normally on the nematic sample, the optical path difference Δl between the ordinary and extraordinary ray is given by

$$\Delta l=\frac{1}{\Lambda}\int_{-\Lambda/2}^{+\Lambda/2}\int_{-d/2}^{+d/2}\Delta n(\phi)dx\,dz=\tfrac{1}{2}n_o R d\langle\phi^2\rangle \ ,$$

where

$$\langle\phi^2\rangle=\frac{1}{d\Lambda}\int_{-\Lambda/2}^{+\Lambda/2}\int_{-d/2}^{+d/2}\phi^2(x,z)dx\,dz \quad (5)$$

is the average square tilt angle, evaluated over a typical length Λ, characterizing the x variation of the surface tilt angle. Furthermore, $R=1-(n_o/n_e)^2$, and n_o and n_e are the ordinary and extraordinary refractive indices, respectively. We point out that the analysis of the nematic properties is usually performed by means of an optical method in which the optical path difference is used to deduce the actual surface nematic orientations. When the surface orientations are known it is possible [10] to measure the anchoring energy.

Typical important cases of surface misalignment are the following.

(i) $\phi_-(x)=\phi_+(x)=\phi_0+A\cos(qx)$,

representing two surfaces whose easy axis is a simple periodic function of x, of wavelength $\lambda=2\pi/q$, around ϕ_0 of amplitude A. ϕ_0 can be considered as the average easy axis. Case (i) is relevant to a sample made of two surfaces of the same kind perfectly in phase. We note that in the case of $A=0$ the tilt angle inside the sample is expected to be constant and equal to ϕ_0.

(ii) $\phi_-(x)=\phi_0+A\cos(qx)$,

$\phi_+(x)=\phi_0+A\cos(qx+\delta)$

similar to the preceding case, but in which the surfaces are out of phase of δ.

(iii) $\phi_-(x)=-\phi_0-A\cos(qx)$,

$\phi_+(x)=\phi_0+A\cos(qx+\delta)$,

which refer to two surfaces in "antisymmetric" arrangement, perfectly in phase for $\delta=0$. In this case, important for practical application, for $A=0$, and strong anchoring, $\phi(x,z)$ is expected to be $\phi(x,z)=2\phi_0 z/d$.

(iv) $\langle\phi_\pm(x)\rangle=\pm\phi_0$,

$\langle\phi_-(x)\phi_-(x')\rangle=\langle\phi_+(x)\phi_+(x')\rangle=AK(x-x')$,

$\langle\phi_-(x)\phi_+(x')\rangle=0$,

representing two surfaces characterized by an average orientation equal to $\pm\phi_0$ varying in a stochastic manner along x. In (iv), A is the amplitude of the stochastic variation and $K(x-x')$ the autocorrelation function.

III. ANALYSIS OF A PERIODIC NOISE ON THE NEMATIC ORIENTATION

As an example, let us consider the case (i) of the preceding section in the strong-anchoring situation

($W\to\infty, L\to 0$). As it is easy to show, solution of Eq. (2) satisfying boundary conditions (4) for the present case is

$$\phi(x,z)=\phi_0+A\cos(qx)\frac{\cosh(qz)}{\cosh(qd/2)} . \tag{6}$$

Consequently, according to (5) the average square tilt angle is

$$\langle\phi^2(x,z)\rangle=\phi_0^2+(\Delta\phi^2)$$

where

$$(\Delta\phi^2)_S=\frac{A^2}{4}\left[\frac{1+\left[\frac{\sinh(qd)}{qd}\right]}{\cosh^2(qd/2)}\right] . \tag{7}$$

In (7) the subscript S means that we are considering the strong-anchoring case. In the following the subscript W will be used when the weak anchoring is analyzed. It follows that the $[\langle\phi^2(x,z)\rangle-\phi_0^2]$ introduced by the fluctuations of the easy tilt angle is given by $(\Delta\phi^2)_S$, whose trend versus d is shown in Fig. 2. From Fig. 2 one deduces that the influence of the fluctuations is important for $qd\sim 1$, i.e., for $\lambda\sim d$. The two important limits for very large and very small thickness of the sample are $qd\to\infty$, $(\Delta\phi^2)_S=0$ and $qd\to 0$, $(\Delta\phi^2)_S=A^2/2$.

The symmetric situation considered above in the case of weak anchoring gives for $\phi(x,z)$ an expression similar to (6) in which A is replaced by $A'=A/[1+qL\tanh(qd/2)]$. Consequently, for the weak-anchoring case $(\Delta\phi^2)_W=(\Delta\phi^2)_S/[1+qL\tanh(qd/2)]^2$, showing that not only d but also L has to be compared with q (see Fig. 2).

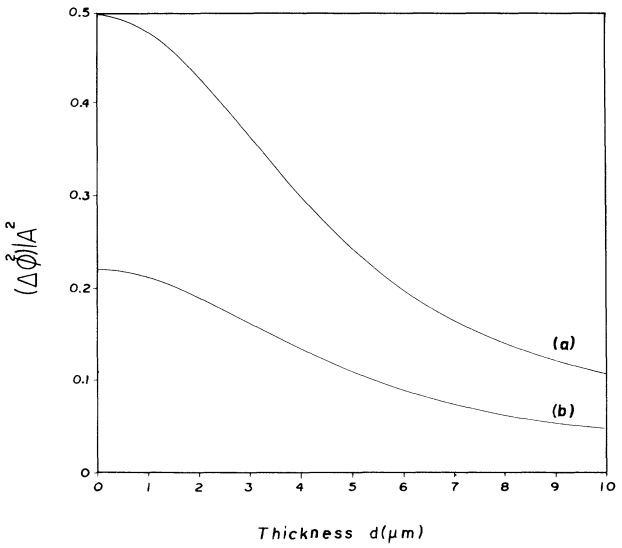

FIG. 2. (a) $(\Delta\phi^2)_S/A^2$ in the strong anchoring case ($L=0$) vs qd. Note that for $qd\sim 1$, $(\Delta\phi^2)_S/A^2\sim 0.42$, and for $qd\to\infty$, $(\Delta\phi^2)_S/A^2\to 0$. The effect of the surface fluctuations of the easy axis is negligible for large thickness of the sample. The curve refers to a situation in which $q=0.5\ \mu m^{-1}$. (b) $(\Delta\phi^2)_W/A^2$ in the weak anchoring case. For large d, $(\Delta\phi^2)_W\sim(\Delta\phi^2)_S/(1+qL)^2$. The curve is drawn for $q=0.5\ \mu m^{-1}$ and $L=1\ \mu m$.

IV. GENERAL SOLUTION OF THE ELASTIC PROBLEM

The other cases reported (ii) and (iii) can be analyzed in a way similar to the one reported in the preceding section. However, in order to study the influence of a stochastic variation of $\Phi_\pm(x)$ on $\langle\phi^2(x,z)\rangle$, it is necessary to develop a general theory giving $\phi(x,z)$ in terms of $\Phi_\pm(x)$. As it is well known, this can be accomplished by introducing the propagator relevant to Eq. (2) and boundary conditions (3) or (4), according to the weak- or strong-anchoring case. In the strong-anchoring case this problem is called Dirichlet's problem, whereas in the case of weak anchoring it is termed mixed Dirichlet-Neumann's problem [14].

By expanding $\phi(x,z)$, in terms of plane waves along x, we have

$$\phi(x,z)=\int_{-\infty}^{+\infty}[\alpha(k)e^{ikx+kz}+\beta(k)e^{ikx-kz}]dk , \tag{8}$$

where $\alpha(k)$ and $\beta(k)$ have to be determined by using the boundary conditions

$$\Phi_\pm(x)=\phi\left[x,\pm\frac{d}{2}\right] , \tag{9}$$

where $\phi_\pm(x)$ are the actual values of $\phi(x,z)$ at the boundaries. They will coincide with $\Phi_\pm(x)$ only in the strong-anchoring case. By substituting (8) in (9) and using the orthonormality of the set $\{e^{ikx}\}$ we obtain

$$\begin{aligned} I_\pm&=\frac{1}{2\pi}\int_{-\infty}^{+\infty}e^{-ikx}\phi_\pm(x)dx \\ &=\alpha(k)e^{\pm k(d/2)}+\beta(k)e^{\mp k(d/2)} , \end{aligned} \tag{10}$$

giving

$$\begin{aligned} \alpha(k)&=\frac{I_+e^{k(d/2)}-I_-e^{-k(d/2)}}{2\sinh(kd)} , \\ \beta(k)&=\frac{I_-e^{k(d/2)}-I_+e^{-k(d/2)}}{2\sinh(kd)} . \end{aligned} \tag{11}$$

By substituting (11) in (8) one has

$$\begin{aligned} \phi(x,z)=\int_{-\infty}^{+\infty}dx'\{&G_+(x-x',z)\phi_+(x') \\ &+G_-(x-x',z)\phi_-(x')\} , \end{aligned} \tag{12}$$

where

$$G_\pm(x-x',z)=\pm\int_{-\infty}^{+\infty}e^{ik(x-x')}\frac{\sinh[k(z\pm d/2)]}{\sinh(kd)}dk . \tag{13}$$

The integral present in (13) can be easily performed, giving for the propagators

$$G_\pm(x-x',z)=\pm\frac{1}{2d}\frac{\cos\left[\frac{\pi}{d}z\right]}{\cosh\left[\frac{\pi}{d}(x-x')\right]\mp\sin\left[\frac{\pi}{d}z\right]} . \tag{14}$$

Equation (12), taking into account (14), gives the general solution of the harmonic problem in terms of the actual values of the functions at the boundaries. In the strong-anchoring case, according to (4), the solution of our problem is

$$\phi(x,z)=\int_{-\infty}^{+\infty}dx'\{G_+(x-x',z)\Phi_+(x') +G_-(x-x',z)\Phi_-(x')\} . \quad (15)$$

On the contrary, in the weak-anchoring case (12) has to be substituted in (3), giving

$$\pm L\int_{-\infty}^{+\infty}dx'\left\{\phi_+(x')\frac{\partial G_+(x-x',z)}{\partial z} +\phi_-(x')\frac{\partial G_-(x-x',z)}{\partial z}\right\}_{z=\pm d/2}+\phi_\pm(x) =\Phi_\pm(x) . \quad (16)$$

Equation (16) constitutes a system of two coupled Fredholm's integral equations in $\phi_\pm(x)$ [14]. In the case in which W is strong enough, and hence L is a small quantity (with respect to the sample thickness and the wavelength of the surface structure), system (16) can be solved by successive approximation. At the first order in L, the solutions are

$$\phi_\pm(x)=\Phi_\pm(x) \pm L\int_{-\infty}^{+\infty}dx'\left[\Phi_+(x')\frac{\partial G_+(x-x',z)}{\partial z} +\Phi_-(x')\frac{\partial G_-(x-x',z)}{\partial z}\right]_{z=\pm d/2} . \quad (17)$$

At this point the problem is formally solved. In Sec. V, we will apply the general formalism to investigate the cases (ii)–(iv) listed at the end of Sec. II.

V. PARTICULAR CASES

Let us now consider the case (ii) of Sec. II in which the "symmetric" case is out of phase of δ. In the strong-anchoring case, Eq. (15) gives

$$\phi(x,z)=\phi_0+\frac{A}{\sinh(qd)}\left\{\sinh\left[q\left[\frac{d}{2}-z\right]\right]\cos(qx) +\sinh\left[q\left[\frac{d}{2}+z\right]\right] \times\cos(qx+\delta)\right\} , \quad (18)$$

which reduces obviously to the previous one in the case of $\delta=0$. Simple calculations give for $(\Delta\phi^2)_S$ the expression

$$(\Delta\phi^2)_S=\frac{A^2}{4\cosh^2\left[q\frac{d}{2}\right]}\frac{\cos(\delta)\left[1+2\sinh^2\left[q\frac{d}{2}\right]\right]-1}{2\sinh^2\left[q\frac{d}{2}\right]} \times\left[1+\frac{\sinh(qd)}{qd}\frac{\cosh(qd)-\cos\delta}{\cos(\delta)\cosh(qd)-1}\right] , \quad (19)$$

whose trend is shown in Fig. 3. In the case in which the anchoring is weak, the solution of our problem is

$$\phi(x,z)=\phi_0+A\left[\frac{\cos\left[\frac{\delta}{2}\right]\cosh(qz)\cos\left[qx+\frac{\delta}{2}\right]}{\left[qL\sinh\left[q\frac{d}{2}\right]+\cosh\left[q\frac{d}{2}\right]\right]} -\frac{\sin\left[\frac{\delta}{2}\right]\sinh(qz)\sin\left[qx+\frac{\delta}{2}\right]}{\left[qL\cosh\left[q\frac{d}{2}\right]+\sinh\left[q\frac{d}{2}\right]\right]}\right] , \quad (20)$$

from which

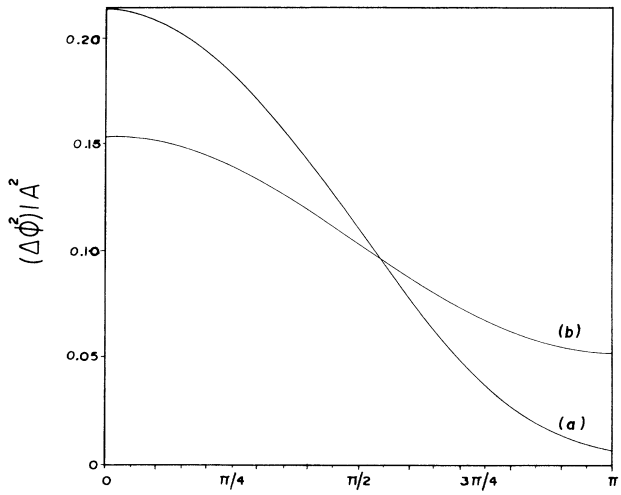

FIG. 3. (a) The effect of the phase on $(\Delta\phi^2)_S$ for the "symmetrical" arrangement in the strong anchoring case for $q=0.5\ \mu m^{-1}$ and $d=4\ \mu m$. (b) The effect of the phase on $(\Delta\phi^2)_W$ in the weak anchoring case for $q=0.5\ \mu m^{-1}$, $d=4\ \mu m$, and $L=1\ \mu m$.

$$(\Delta\phi^2)_W=\frac{A^2}{4}\left[\frac{\cos^2\left[\frac{\delta}{2}\right]\left[1+\frac{\sinh(qd)}{qd}\right]}{\left[qL\sinh\left[q\frac{d}{2}\right]+\cosh\left[q\frac{d}{2}\right]\right]^2}+\frac{\sin^2\left[\frac{\delta}{2}\right]\left[-1+\frac{\sinh(qd)}{qd}\right]}{\left[qL\cosh\left[q\frac{d}{2}\right]+\sinh\left[q\frac{d}{2}\right]\right]^2}\right], \tag{21}$$

showing again, that q has to be compared not only with d, but also with L (Fig. 3).

The case (iii) of antisymmetric period axis, connected to $\delta=0$, for the strong-anchoring case, is characterized by a profile of tilt angle of the kind

$$\phi(x,z)=\frac{2\phi_0 z}{d}+A\frac{\sinh(qz)}{\sinh\left[q\frac{d}{2}\right]}\cos(qx)\ . \tag{22}$$

In the case in which $A=0$ we obtain the profile well known in the literature

$$\phi_u(z)=\frac{2\phi_0 z}{d}\ . \tag{23}$$

In the uniform case (23), trivial calculations give

$$\langle\phi_u^2\rangle=\tfrac{1}{3}\phi_0^2\ . \tag{24}$$

In the general case, by using (22) one obtains

$$(\Delta\phi^2)_S=\langle\phi^2\rangle-\langle\phi_u^2\rangle=\frac{A^2}{2}\left[\frac{-1+\frac{\sinh(qd)}{qd}}{\cosh(qd)-1}\right], \tag{25}$$

shown in Fig. 4. To complete the investigation of this antisymmetric arrangement, characterized by $\delta=0$, it remains to evaluate the situation in which the anchoring is weak. In this case Eqs. (15) and (17) give again expression (22), where instead of ϕ_0 and A we have to replace $\tilde{\phi}_0$ and $\tilde{A}$ with

$$\tilde{\phi}_0=\frac{1}{d+2L}\phi_0 \tag{26}$$

and

$$\tilde{A}=\frac{A}{1+qL\coth\left[q\frac{d}{2}\right]}\ , \tag{27}$$

$(\Delta\phi^2)_W$ can be straightforwardly evaluated and it is found to be

$$(\Delta\phi^2)_W=\frac{(\Delta\phi^2)_S}{\left[1+qL\coth\left[q\frac{d}{2}\right]\right]^2} \tag{28}$$

and it is shown in Fig. 4.

The antisymmetric case out of phase of δ is described, in the strong anchoring case, by a profile tilt angle given by

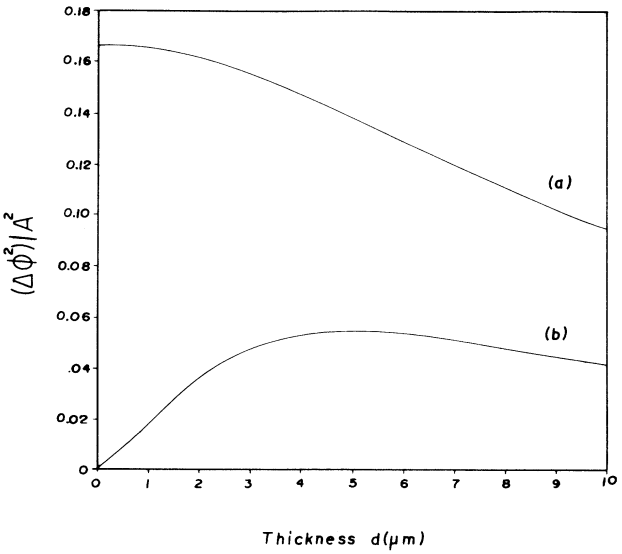

FIG. 4. (a) $(\Delta\phi^2)_W/A^2$ vs d for the "antisymmetric" arrangement in the strong anchoring situation ($q=0.5\ \mu\text{m}^{-1}$). (b) $(\Delta\phi^2)_W/A^2$ vs d for the antisymmetric arrangement in the weak-anchoring situation $q=0.5\ \mu\text{m}^{-1}$ and $L=1\ \mu$m.

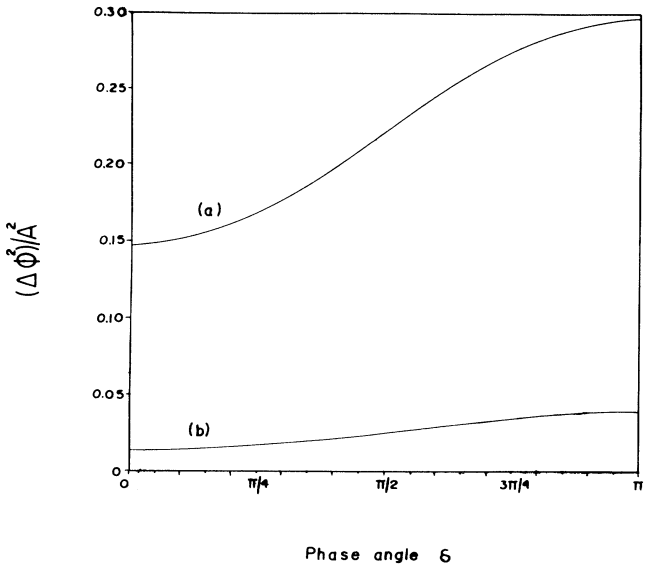

FIG. 5. (a) $(\Delta\phi^2)/A^2$ vs the phase δ for $q=0.5\ \mu\text{m}^{-1}$ and $d=4\ \mu$m. (a) Strong-anchoring case; (b) weak-anchoring case ($L=1\ \mu$m).

$$\phi(x,z)=\frac{2\phi_0 z}{d}+\frac{A}{\sinh(qd)}\left\{-\sinh\left[q\left[\frac{d}{2}-z\right]\right]\cos(qx)+\sinh\left[q\left[\frac{d}{2}+z\right]\right]\cos(qx+\delta)\right\}. \tag{29}$$

Consequently,

$$(\Delta\phi^2)_S=\frac{A^2}{2[\cosh(qd)-1]}\left[\frac{-[1+\cos(\delta)\cosh(qd)]+\frac{\sinh(qd)}{qd}[\cosh(qd)+\cos\delta]}{1+\cosh(qd)}\right], \tag{30}$$

which reduces to (25) when $\delta=0$. This case, in the weak-anchoring situation, is characterized by a tilt angle of the kind

$$\phi(x,z)=\frac{2\phi_0 z}{d+2L}+A\left\{\frac{\cos\left[\frac{\delta}{2}\right]\sinh(qz)\cos\left[qx+\frac{\delta}{2}\right]}{qL\cosh\left[q\frac{d}{2}\right]+\sinh\left[q\frac{d}{2}\right]}-\frac{\sin\left[\frac{\delta}{2}\right]\cosh(qz)\sin\left[qx+\frac{\delta}{2}\right]}{qL\sinh\left[q\frac{d}{2}\right]+\cosh\left[q\frac{d}{2}\right]}\right\} \tag{31}$$

from which one obtains for $(\Delta\phi^2)_W$ the expression

$$(\Delta\phi^2)_W=\frac{1}{3}\phi_0^2\left[\frac{d}{d+2L}\right]^2+\frac{A^2}{4}\left[\frac{\cos^2\left[\frac{\delta}{2}\right]\left[-1+\frac{\sinh(qd)}{qd}\right]}{\left[qL\cosh\left[q\frac{d}{2}\right]+\sinh\left[\frac{qd}{2}\right]\right]^2}+\frac{\sin^2\left[\frac{\delta}{2}\right]\left[1+\frac{\sinh(qd)}{qd}\right]}{\left[qL\sinh\left[q\frac{d}{2}\right]+\cosh\left[q\frac{d}{2}\right]\right]^2}\right], \tag{32}$$

shown in Fig. 5 (apart from a constant factor). To complete our analysis, in Sec. VI a random fluctuation around the mean value will be considered.

VI. EFFECT OF RANDOM EASY AXIS FLUCTUATIONS ON THE BULK PROPERTIES

In this section the effect of a random fluctuation is analyzed. First the case of strong anchoring will be considered. In this situation the actual tilt angle is given by the general expression (15). Let us consider the symmetric situation in which $\Phi_\pm(x')=\phi_0+\epsilon_\pm(x')$ where $\epsilon_\pm(x)$ will be assumed a random function. By using (15) the average along x of $\phi^2(x,z)$ is given by

$$\begin{aligned}\langle\phi^2(x,z)\rangle_x&=\frac{1}{\Lambda}\int_{-\Lambda/2}^{\Lambda/2}\phi^2(x,z)dx\\&=\phi_0^2+\frac{1}{\Lambda}\int_{-\infty}^{+\infty}\int_{-\infty}^{+\infty}g_{ij}(x'-x'',z)\epsilon_i(x')\\&\quad\times\epsilon_j(x'')dx'dx''\end{aligned} \tag{33}$$

where the new propagators are defined as

$$\begin{aligned}g_{ij}(x'-x'',z)&=\int_{-\Lambda/2}^{\Lambda/2}G_i(x'-x,z)G_j(x''-x,z)dx\\&=g_{ij}(x''-x',z)\end{aligned} \tag{34}$$

and they are explicitly evaluated in the Appendix. In order to save space, in (33) and in the following, we use the summation convention and put $i=+,-$. Because the integrand in (34) is strongly decreasing when x increases, it is possible to extend the integration by supposing $\Lambda\to\infty$. In this way the propagator (34) is completely defined. Let us suppose now that $\langle\epsilon_i(x')\rangle=0$, $\langle\epsilon_i(x')\epsilon_j(x'+s)\rangle=A^2K(s)\delta_{ij}$, where the averages are evaluated over the typical scale Λ, and A is the maximum amplitude of $\epsilon(x)$. $K(s)$ is the autocorrelation function and we suppose that the orientations on the two surfaces are uncorrelated, as already pointed out in Sec. II. In this frame, one obtains for the second and third terms appearing in (33), after the substitution $x''=x'+s$,

$$\begin{aligned}&\frac{1}{\Lambda}\int_{-\infty}^{\infty}\int_{-\infty}^{\infty}g_{ij}(x'-x'',z)\epsilon_i(x')\epsilon_j(x'')dx'dx''\\&\quad=\int_{-\infty}^{+\infty}ds\,g_{ij}(s,z)\left[\frac{1}{\Lambda}\int_{-\infty}^{+\infty}\epsilon_i(x')\epsilon_j(x'+s)dx'\right]\\&\quad=A^2\delta_{ij}\int_{-\infty}^{+\infty}K(s)g_{ij}(s,z)ds\ .\end{aligned}$$

It follows that

$$\langle\phi^2(x,z)\rangle=\phi_0^2+A^2\int_{-\infty}^{+\infty}K(s)\tilde{G}_{ii}(s)ds\ , \tag{35}$$

where

$$\tilde{G}_{ii}(s)=\frac{1}{d}\int_{-d/2}^{d/2}g_{ii}(s,z)dz \tag{36}$$

is the average along z of the new propagator defined in (34). In the case in which $K(s)=\Lambda\delta(s)$ (white noise [15]), the integration appearing in (35) can be easily performed giving,

$$(\Delta\phi^2)=\Lambda A^2\tilde{G}_{ii}(0)\ . \tag{37}$$

The other case, in which $\Phi_{\pm}(x)=\pm\phi_0\pm\epsilon_{\pm}(x)$, called before the antisymmetric arrangement, can be analyzed in the same way. The final result in the strong-anchoring situation is

$$\langle\phi^2(x,z)\rangle=\tfrac{1}{3}\phi_0^2+A^2\int_{-\infty}^{+\infty}K(s)\tilde{G}_{ii}(s)ds\ , \tag{38}$$

which, in the case of white noise, is written again in the form (37). The case of weak anchoring can be treated in a similar way by using Eq. (17), but it will not be analyzed here because the calculations are very ponderous and they do not add any new physical information.

In order to show the importance of the results obtained in this section, we discuss now the physical consequences of the noise on the easy axis on the experimental observations. Let us consider an experimental situation in which, by means of an optical technique, an experimentalist tries to determine the anchoring energy as described in [16]. Let us suppose that the surface treatment ensures an orientation of the kind $\Phi_{\pm}(x)=\phi_0+\epsilon_{\pm}(x)$ characterized by strong anchoring. In order to detect ϕ_0, the experimentalist has to put the surface in symmetric arrangement. As shown before, in this manner the experimentalist measures, by means of the optical path difference, the quantity

$$\langle\phi^2_{\rm sym}(x,z)\rangle=\phi_0^2+(\Delta\phi^2)_{\rm sym}=\phi_0'^2 \tag{39}$$

where $(\Delta\phi^2)$, as follows from Eq. (35), is given by

$$(\Delta\phi^2)=A^2\int_{-\infty}^{+\infty}K(s)\tilde{G}_{ii}(s)ds\ . \tag{40}$$

When one puts the surfaces in antisymmetric arrangement the measured quantity is

$$\langle\phi^2_{\rm anti}(x,z)\rangle=\tfrac{1}{3}\phi_0^2+(\Delta\phi^2)_{\rm anti}=\tfrac{1}{3}\phi_0''^2 \tag{41}$$

giving

$$\phi_0''=[\phi_0^2+3(\Delta\phi^2)_{\rm anti}]^{1/2}\ , \tag{42}$$

in which $(\Delta\phi^2)_{\rm anti}=(\Delta\phi^2)_{\rm sym}$, in the case considered (see above). The connection between ϕ_0'',ϕ_0' and the anchoring energy is [16]

$$\phi_0''=\phi_0'\Big/\left[1+2\frac{L}{d}\right] \tag{43}$$

where L is connected to the apparent anchoring energy. By using (39) and (43) one obtains

$$1+2\left[\frac{L}{d}\right]=\left[\left\{1+\frac{(\Delta\phi^2)_{\rm sym}}{\phi_0^2}\right\}\Big/\left\{1+3\frac{(\Delta\phi^2)_{\rm anti}}{\phi_0^2}\right\}\right]^{1/2}, \tag{44}$$

giving

$$\frac{L}{d}\cong\frac{1}{4}\left[\frac{(\Delta\phi^2)_{\rm sym}}{\phi_0^2}-3\frac{(\Delta\phi^2)_{\rm anti}}{\phi_0^2}\right] \tag{45}$$

if $(\Delta\phi^2)/\phi_0^2\ll1$. Equation (44) shows that a random fluctuation of the easy axis can be interpreted as a weak-anchoring situation, although the true anchoring is strong. The calculations performed above in the general case for an easy axis varying along x in stochastic way hold for $(\Delta\phi^2)/\phi_0^2\ll1$. The same analysis, relevant to a simple periodic variation of the easy axis along x, can be done by using Eqs. (39) and (41) in which $(\Delta\phi^2)_{\rm sym}$ and $(\Delta\phi^2)_{\rm anti}$ are given by (7) and (25), respectively. In this manner, Eq. (44) gives for the apparent extrapolation length, the expression

$$L=\frac{1}{2}d\left\{\left[\frac{1+\frac{1}{4}\left[\frac{A}{\phi_0}\right]^2\frac{1+\frac{\sinh(qd)}{qd}}{\cosh^2\left[\frac{qd}{2}\right]}}{1+\frac{3}{4}\left[\frac{A}{\phi_0}\right]^2\frac{-1+\frac{\sinh(qd)}{qd}}{\sinh^2\left[q\frac{d}{2}\right]}}\right]^{1/2}-1\right\}, \tag{46}$$

valid in general. The trend of L/d vs d for this case is drawn in Fig. 6 for different values of $(A/\phi_0)^2$. Note that for $qd\to0$ and $(A/\phi_0)^2\sim1$, this equation gives $L/d\to0$, in agreement with the general formula (45). In the case of white noise, Eq. (45) becomes

$$\frac{L}{d}=-\frac{1}{2}\Lambda A^2\tilde{G}_{ii}(0)\ . \tag{47}$$

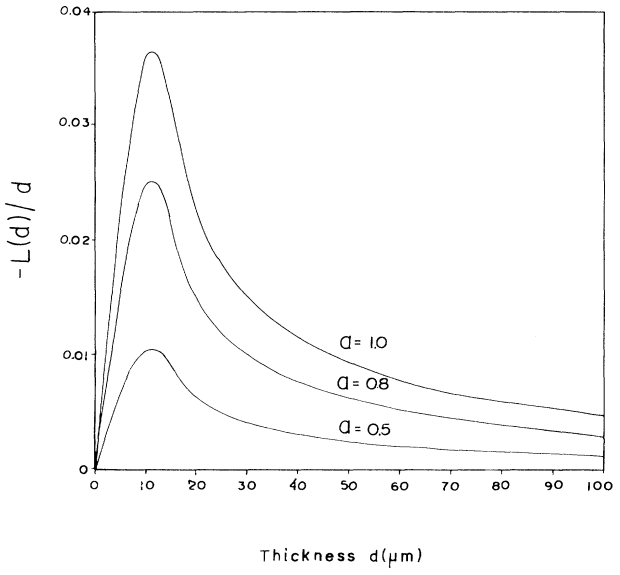

FIG. 6. Trend of $-L(d)/d$ vs d for a sample characterized by two surfaces in antisymmetric arrangement perfectly in phase with easy axis varying in a simple periodic way having strong anchoring for $a=A/\phi_0=0.5,0.8,1.0$. Note that for $d\to0$, $L/d\to0$, and for $d\to\infty$, $L/d\to0$. The two limits are easily understood. In fact, if $d\ll q$, the local orientation depends only on the surface, which can be considered uniform. In the other limit, since the nonuniformity is completely lost, the anchoring is strong again.

In order to have an idea about the order of magnitude of the estimated extrapolation length, we note that $\tilde{G}_{ii}(0)\alpha 1/d$ (as shown in the Appendix) or, more precisely, $\tilde{G}_{ii}(0)d=1/2\pi$. Hence $L/\Lambda=-A^2/4\pi$. It follows that, as expected, L is of the order of the "periodicity" of the easy axis along x.

VII. CONCLUSIONS

The effect of a fluctuation of easy axis imposed by a surface treatment on the bulk properties of a nematic liquid crystal has been evaluated. Our analysis, performed in the cases of strong and weak anchoring has shown that a surface fluctuation in the average orientation may be interpreted as a weak anchoring, even in the case in which the surface treatment is characterized by strong anchoring. We have analyzed several cases, important from a practical point of view. The effect is usually important in all the situations in which the surface periodicity is comparable with the thickness of the sample. Consequently, before detecting experimentally the surface energy, the experimentalists have to estimate the surface periodicity of the surface tilt angle; otherwise their results have to be reanalyzed. In our paper we have supposed that the wavelength of the surface periodicity is very large with respect to the nematic coherence length. If this condition is not fulfilled, it is no longer possible to employ the elastic energy written in the simple Frank form and the analysis is much more complicated [17].

ACKNOWLEDGMENTS

Many thanks are due to T. Beica (IFTM, Bucharest), G. Durand (Laboratoire de Physique des Solides, Orsay), A. L. Alexe-Ionescu (Polytechnical Institute, Bucharest), R. Moldovan (IFTM, Bucharest), and A. K. Zvezdin (Institute of General Physics, Moscow) for useful discussions. This work was partially supported by bilateral cooperation between Departmento de Fisica-FUEM and Dipartmento di Fisica del Politecnico di Torino.

APPENDIX

The propagator g_{++} is defined by (34). In order to evaluate the integral appearing in that expression, let us put

$$\alpha=\tfrac{1}{2}\cosh(2u)+\sin^2\nu,\quad \beta=2\sin(\nu)\cosh(u)$$

where $u=(\pi/d)(x'-x'')$ and $\nu=(\pi/d)z$. In this way, $g_{++}(u,\nu)$ can be rewritten as

$$g_{++}(u,\nu)=\frac{\cos^2\nu}{4\pi d}\int_{-\infty}^{+\infty}\frac{d\xi}{\left[\alpha+\frac{1}{2}\cosh\xi-\beta\cos\frac{\xi}{2}\right]}$$

where $\xi=2(\pi/d)x$. The integration in the above formula may be performed in elementary way [18]. The final result is

$$g_{++}(u,\nu)=\frac{\cos\nu}{8\pi d\sinh(u)[\cos^2(\nu)\cosh^2u+\sin^2(\nu)\sinh^2u]}\times\left\{\cos(\nu)\cosh(u)\ln\left[\frac{\sin^2(2\nu)+(2\cos^2\nu+e^{2u}-1)^2}{\sin^2(2\nu)+(2\cos^2\nu+e^{-2u}-1)^2}\right]-2\sin(\nu)\sinh(u)h(u,\nu)\right\},$$

where

$$h(u,\nu)=\left\{\left[\tan^{-1}\left[\frac{\sin^2(2\nu)+(2\cos^2\nu+e^{2u}-1)^2}{2\sin(2\nu)}\right]+\tan^{-1}\left[\frac{\sin^2(2\nu)+(2\cos^2\nu+e^{-2u}-1)^2}{2\sin(2\nu)}\right]\right]\right\}.$$

The function g_{++} is strongly peaked around $u=0$.

*Permanent address: Dipartimento di Fisica, Politecnico di Torino, Corso Duca degli Abruzzi, 24, 10129 Torino, Italy. Present address: Laboratoire de Physique des Solides, Université de Paris–Sud, Bâtiment 510, 91405 Orsay Cedex, France.

[1] P. G. de Gennes, *The Physics of Liquid Crystals* (Clarendon, Oxford, 1974).
[2] E. B. Priestley, P. G. Wojtowickz, and Ping Sheng, *Introduction to Liquid Crystals* (Plenum, New York, 1975).
[3] S. Chandrasekhar, *Liquid Crystals* (Cambridge University Press, Cambridge, 1977).
[4] F. C. Frank, Discuss. Faraday Soc. **25**, 19 (1958).
[5] G. Durand (unpublished); Liq. Cryst. (to be published).
[6] G. Durand, in Proceedings of the Les Houches Summer School: Session XLVIII Liquids at Interfaces, edited by J. Charvolin, J. F. Joanny, and J. Zinn-Justin (North-Holland, Amsterdam, 1990), p. 633.
[7] N. V. Madhusudana and G. Durand, J. Phys. Lett. (Paris) **46**, 195 (1985).
[8] W. H. de Jeu, *Physical Properties of Liquid Crystal Materials: Liquid Crystal Monograph,* Vol. I (Gordon and Breach, London, 1980).
[9] S. Faetti, Mol. Cryst. Liq. Cryst. **179**, 217 (1990).
[10] G. Barbero, N. V. Madhusudana, and G. Durand, Z. Naturforsch. **392**, 1066 (1984).
[11] A. Rapini and M. Papoular, J. Phys. (Paris) Colloq. **30**, C4-54 (1969).
[12] I. V. Smirnov, *Cours de Mathematiques Superieurs* (Mir, Moscow, 1976), Vol. IV.
[13] M. Kleman, *Points, Lignes, Parois* (Les Editions de Phy-

sique, Les Ulis, 1976).
[14] P. M. Morse and H. Feshbach, *Methods of Theoretical Physics* (McGraw-Hill, New York, 1953), Vol. I.
[15] R. K. Pathria, *Statistical Mechanics* (Pergamon, Oxford, 1972).
[16] L. Komitov and A. G. Petrov, Phys. Status Solidi **76**, 137 (1983).
[17] G. Barbero and G. Durand, J. Appl. Phys. **67**, 2678 (1990).
[18] I. S. Gradshteyn and I. M. Ryzhik, *Tables of Integrals, Series and Products* (Academic, New York, 1965).